Nuclear Physics **A491** (1989) 1–23
North-Holland, Amsterdam

EMPIRICAL ISOSPIN-NONCONSERVING HAMILTONIANS FOR SHELL-MODEL CALCULATIONS

W.E. ORMAND[1]

NORDITA and The Niels Bohr Institute, Blegdamsvej 17, DK-2100 Copenhagen Ø, Denmark

B.A. BROWN

National Superconducting Cyclotron Laboratory
and
Department of Physics and Astronomy,
Michigan State University, East Lansing, MI 48824-1321, USA

Received 12 October 1987
(Revised 6 July 1988)

Abstract: Hamiltonians for shell-model calculations of isospin-nonconserving (INC) processes are determined empirically by requiring that they reproduce experimentally measured isotopic mass shifts. Five separate configuration spaces were considered: the 0p; the $0p_{1/2}$, $0d_{5/2}$, and $1s_{1/2}$; the 1s-0d; the $0d_{3/2}$ and $0f_{7/2}$; and the 0f-1p shell-model spaces. The INC hamiltonian was assumed to be comprised of the Coulomb force plus phenomenological isospin-nonconserving nucleon-nucleon interactions. The parameters of the hamiltonian are the isovector single-particle energies, the overall Coulomb strength, and the isovector and isotensor strengths of the nucleon-nucleon INC interaction; and were obtained by performing a least-squares fit to experimental b- and c-coefficients of the isobaric-mass-multiplet equation.

1. Introduction

Shortly after the discovery of the neutron, Heisenberg [1]) proposed the existence of a new intrinsic quantum number, isospin, which reflects the symmetry between protons and neutrons, and has since then proven to be a powerful tool for the labeling of nuclear states. The question as to how good a quantum number isospin is depends on the charge symmetry of the nuclear hamiltonian, i.e. if $[\boldsymbol{T}, H] = 0$, then isospin is a conserved quantity. Clearly, the Coulomb interaction between protons breaks the proton-neutron symmetry, and is a source of isospin-symmetry violation. In addition, nucleon-nucleon scattering data suggests that the nucleon-nucleon interaction is slightly nonsymmetric with respect to charge [2]). The scattering lengths in the $T = 1$ channel indicate that the proton-proton and neutron-neutron interactions ($v^{(pp)}$ and $v^{(nn)}$, respectively) are approximately the same within experimental uncertainty, while the proton-neutron interaction ($v^{(pn)}$) is approximately 2% stronger than the average of $v^{(pp)}$ and $v^{(nn)}$. Although the extent to which isospin

[1] Current address: Dipartimento di Fisica, Universitá di Milano, via Celoria 16, and INFN Sezione di Milano, 20133 Milano, Italy.

conservation is violated is small, comparisons between experimentally observed isospin-symmetry violation and theoretical estimates might lead to a further understanding of nuclear structure and the isospin-nonconserving (INC) interaction.

Some experimental measurements where isospin-symmetry violation plays an important role are:

(i) mass shifts between isobaric analog states,

(ii) isospin-forbidden proton and neutron emission, for example, the decay of $T=\frac{3}{2}$ states in $A=4n+1$ nuclei to $T=0$ states [3]),

(iii) isospin-forbidden Fermi β-decays [4]) (Fermi transitions to states that are not analogs of the parent), and

(iv) β-delayed two proton decays of ^{22}Al and ^{26}P [ref. [5])], in which at least one of the observed sequential protons must violate isospin conservation.

Nolen and Schiffer [6]) showed that the Coulomb force alone cannot account for the mass difference between $T=\frac{1}{2}$ analog states. This effect is commonly referred to as the Nolen-Schiffer anomaly, and, at present, has no consensus as to its explanation (for a review see ref. [7])). A small asymmetry between the proton-proton and neutron-neutron interactions can account for at least part of the Nolen-Schiffer anomaly [8-10]). However, although charge asymmetry is not excluded by nucleon-nucleon scattering data, there is no theoretical model for such a force that would systematically account for the mass shifts observed in all nuclei [8-10]). In addition, there is also considerable evidence that the Coulomb force alone cannot account for the isotensor component of the isobaric analog mass shifts of states with $T>\frac{1}{2}$ [refs. [11-14])]. An additional short-ranged proton-neutron interaction is required, whose strength is consistent with the nucleon-nucleon scattering data mentioned above.

The aim of this work is to develop empirical INC interactions that may be used in extended shell-model configuration spaces to calculate the effects of isospin nonconservation in a wide range of nuclei. Our intent is to extend and to improve upon previous works along these lines [11-14]). A hamiltonian comprised of the Coulomb potential plus phenomenological isospin-nonconserving nucleon-nucleon interactions is obtained within the framework of the nuclear shell model for five separate configuration spaces by imposing the constraint that the parameters of these interactions reproduce experimentally determined isostopic mass shifts. With the INC interaction thus determined, it should then be feasible to make theoretical predictions as to the extent to which isospin conservation is violated in nuclei. In addition to processes (ii)-(iv) mentioned above, we are also interested in using our empirical INC interaction to calculate isospin-mixing corrections to the Fermi matrix element in superallowed Fermi β-decay [15]).

This work is organized in the following manner. First, a derivation of the isobaric-mass-multiplet equation (IMME) and the mechanism for evaluating the b- and c-coefficients within the framework of the shell model are given in sect. 2. In sect. 3, the procedure used to determine the isospin-nonconserving hamiltonian for each

shell-model configuration space is outlined, while in subsect. 3.1 and 3.2, the results of the fits to b- and c-coefficients, respectively, are given. A discussion and concluding remarks are given in sect. 4.

2. Isobaric-mass-multiplet equation (IMME)

Wigner [16]) was the first to demonstrate that the mass differences between members of the same isobaric multiplet can be parameterized by

$$E(\nu, T, T_z) = a(\nu, T) + b(\nu, T)T_z + c(\nu, T)T_z^2, \tag{2.1}$$

where the label ν represents all other relevant quantum numbers, including the nuclear mass A. This parameterization is referred to as the isobaric-mass-multiplet equation (IMME), and is derived by noting that the nuclear hamiltonian can be decomposed into isoscalar ($k=0$), isovector ($k=1$), and isotensor ($k=2$) components, i.e.

$$H_{\rm tot} = \sum_{k=0}^{2} H^{(k)}.$$

Since the dominant contribution to the energy is due to the isoscalar part of the hamiltonian, one can start with the states $\psi(\nu, T, T_z)$, which are eigenstates of $H^{(0)}$, and evaluate the energy shift due to the isovector and isotensor components of the hamiltonian using perturbation theory. Applying the Wigner-Eckart theorem [17]), the energy of the state $|\psi(\nu, T, T_z)\rangle$ is then

$$\begin{aligned} E(\nu, T, T_z) &= \langle\psi(\nu, T, T_z)|H_{\rm tot}|\psi(\nu, T, T_z)\rangle \\ &= (2J+1)^{-1/2} \sum_{k=0}^{2} (-1)^{T-T_z} \begin{pmatrix} T & k & T \\ -T_z & 0 & T_z \end{pmatrix} \langle\psi(\nu, T)|||H^{(k)}|||\psi(\nu, T)\rangle, \end{aligned} \tag{2.2}$$

where the three bars denote a reduction in both isospin and angular momentum space. Substituting explicit values for the 3-j coefficients in to eq. (2.2), one obtains

$$E(\nu, T, T_z) = E^{(0)}(\nu, T) + E^{(1)}(\nu, T)T_z + E^{(2)}(\nu, T)(3T_z^2 - T(T+1)), \tag{2.3}$$

where

$$\begin{aligned} E^{(0)}(\nu, T) &= \{(2J+1)(2T+1)\}^{-1/2}\langle\psi(\nu, T)|||H^{(0)}|||\psi(\nu, T)\rangle, \\ E^{(1)}(\nu, T) &= \{(2J+1)T(2T+1)(T+1)\}^{-1/2}\langle\psi(\nu, T)|||H^{(1)}|||\psi(\nu, T)\rangle, \\ E^{(2)}(\nu, T) &= \{(2J+1)(2T-1)(2T+1)(T+1)(2T+3)\}^{-1/2}\langle\psi(\nu, T)|||H^{(2)}|||\psi(\nu, T)\rangle. \end{aligned} \tag{2.4}$$

Eq. (2.3) then has the form of eq. (2.1) with

$$a(\nu, T) = E^{(0)}(\nu, T) - T(T+1)E^{(2)}(\nu, T), \tag{2.5a}$$

$$b(\nu, T) = E^{(1)}(\nu, T), \tag{2.5b}$$

$$c(\nu, T) = 3E^{(2)}(\nu, T). \tag{2.5c}$$

Deviations from the parameterization of the IMME are an indication that higher-order perturbation theory and/or the possibility of three-body interactions must be considered. For states with $T \geqslant \frac{3}{2}$, these effects can be accounted for empirically by adding the term dT_z^3 to eq. (2.1). Twenty-seven isobaric quintets have been analyzed [18,19]) to see if they fit the systematics of the IMME, and in all but two cases ($A=9$ and $A=13$; with d-coefficients of 5.2 ± 1.7 and -3.1 ± 1.9 keV, respectively) the d-coefficients were found to be consistent with zero, with an upper limit on their absolute values being between 5 and 10 keV. This absence of experimental d-coefficients is a strong indication that a first-order perturbation-theory calculation of the isotopic mass differences, which utilizes only two-body interactions, is adequate at the level needed for most quantities of interest.

In this work, the reduced many-body matrix elements of the isospin-nonconserving components of $H_{\rm tot}$, are evaluated within the framework of the nuclear shell model. The starting point of our calculations is the many-body Slater determinants obtained within the usual spherical basis $|\psi(n, l, j)\rangle = R_{nlj}(r)(Y^l \times s)^j$, in which $(A-C)$ nucleons occupy valence orbits outside a spherically closed core of C nucleons. Within this basis, we need to account for two-body interactions between particles occupying the valence orbits as well as with those inside the closed core. The reduced matrix element of $H^{(k)}$ is then [20])

$$\begin{aligned}\langle \psi(\nu, T) \| H^{(k)} \| \psi(\nu, T) \rangle = & \sum_{ij} \mathrm{OBTD}_{\nu,T;\nu,T}(\rho_i, \rho_j; k) \langle \mathrm{core}, \rho_i \| H^{(k)} \| \mathrm{core}, \rho_j \rangle \\ & \sum_{ijmn} \mathrm{TBTD}_{\nu,T;\nu T}(\rho_i \rho_j; \lambda_{ij} : \rho_m \rho_n; \lambda_{mn}; k) \\ & \times \langle \rho_i \rho_j; \lambda_{ij} \| H^{(k)} \| \rho_m \rho_n; \lambda_{mn} \rangle , \end{aligned} \tag{2.6}$$

where the sums are taken over the valence orbits, ρ represents the single-particle quantum numbers nlj and the ket $|\rho_i \rho_j; \lambda_{ij}\rangle$ is an antisymmetric two-nucleon wave function with particles occupying the valence orbits ρ_i and ρ_j, coupled to the intermediate state λ_{ij}, where λ_{ij} is a short-hand notation representing the intermediate angular-momentum and isospin coupling quantum numbers, i.e. J and T, respectively. The reduced one-body matrix element $\langle \mathrm{core}, \rho_i \| H^{(k)} \| \mathrm{core}, \rho_j \rangle$ represents a sum of two-body interactions between particles in the closed core with those occupying the valence orbits (note that for the cases at hand we have $\rho_i = \rho_j$), and is related to the single-particle energy $\varepsilon^{(k)}$ by

$$\varepsilon^{(k)}(\rho_i) = \left(\frac{2}{3(2j_i+1)} \right)^{1/2} \langle \mathrm{core}, \rho_i \| H^{(k)} \| \mathrm{core}, \rho_i \rangle ,$$

where $\varepsilon^{(k)}$ is given in terms of the proton and neutron single-particle energies by

$$\begin{aligned} \varepsilon^{(0)} &= \tfrac{1}{2}(\varepsilon^{(\mathrm{p})} + \varepsilon^{(\mathrm{n})}) , \\ \varepsilon^{(1)} &= \varepsilon^{(\mathrm{p})} - \varepsilon^{(\mathrm{n})} . \end{aligned} \tag{2.7}$$

The general form for the one-body and two-body transition densities (OBTD and TBTD, respectively) are given by [20]*

$$\mathrm{OBTD}_{\Gamma;\Gamma'}(\rho_i,\rho_j;\lambda)=(2\lambda+1)^{-1/2}\langle\psi(\Gamma)\|\{a^{\dagger}_{\rho_i}\times\tilde{a}_{\rho_j}\}^{\lambda}\|\psi(\Gamma')\rangle, \tag{2.8a}$$

$$\begin{aligned}\mathrm{TBTD}_{\Gamma;\Gamma'}(\rho_i,\rho_j;\lambda_{ij}:\rho_m\rho_n;\lambda_{mn};\lambda)=&-\{(2\lambda+1)(1+\delta_{\rho_i\rho_j})(1+\delta_{\rho_m\rho_n})\}^{-1/2}\\ &\times\langle\psi(\Gamma)\|\{(a^{\dagger}_{\rho_i}\times a^{\dagger}_{\rho_j})^{\lambda_{ij}}\\ &\times(\tilde{a}_{\rho_m}\times\tilde{a}_{\rho_n})^{\lambda_{mn}}\}^{\lambda}\|\psi(\Gamma')\rangle,\end{aligned} \tag{2.8b}$$

where Γ represents all relevant quantum numbers, and $a^{\dagger}_{\rho}$ and $\tilde{a}_{\rho}$ are tensor operators that create and annihilate a nucleon in the ρth orbit, respectively. The intermediate couplings λ_{ij} and λ_{mn} are restricted by the requirement that the final coupling λ must have angular momentum $\Delta J=0$ and isospin $\Delta T=k$, and the factor $(2\lambda+1)^{-1/2}$ is shorthand for $[(2\Delta J+1)(2\Delta T+1)]^{-1/2}$.

A perturbative calculation of the isotopic mass differences with the framework of the shell model can then be used to determine an empirical INC interaction in the following manner. First, the one-body and two-body transition densities are evaluated using the wave functions $\psi(\nu,T)$ obtained from a suitable isoscalar hamiltonian. Then an INC interaction comprised of the Coulomb potential plus a phenomenological INC nucleon–nucleon interaction is assumed (see eq. (3.1) below). The only quantities that then need to be determined are the isovector single-particle energies and the strength coefficients for each component of the INC interaction. These parameters are determined by performing a least-squares fit to a set of experimental b- and c-coefficients.

3. Determination of the INC interaction

The starting point of our calculation of the b- and c-coefficients is the shell-model wave functions $\psi(\nu,T)$ (the label T_z is unnecessary, as the matrix elements evaluated with these wave functions are reduced in isospin space) that are eigenstates of the isoscalar hamiltonian. Due to the wide range of nuclei ($10\leq A\leq 55$) that are of interest, five separate configuration spaces and isoscalar hamiltonians were considered in this work. These are:

(i) $0p_{3/2}$ and $0p_{1/2}$ orbits (0p model space) and the interaction of Cohen and Kurath [21]) (CKPOT),

(ii) $0p_{1/2}$, $0d_{5/2}$, and $1s_{1/2}$ orbits (pds model space) and the interaction of Reehal and Wildenthal [22]) (RW),

(iii) $0d_{5/2}$, $1s_{1/2}$, and $0d_{3/2}$ orbits (1s-0d model space) and the mass-dependent sd-shell interaction of Wildenthal [23]) (W),

(iv) $0d_{3/2}$ and $0f_{7/2}$ orbits (df model space) and the interaction of Hsieh, Mooy, and Wildenthal [24]) (HMW), and

* Note that in ref. [20]) the second and third lines of eq. (14.60) should be divided by $[(1+\delta_{\rho_1\rho_2})\times(1+\delta_{\rho_3\rho_4})]^{1/2}$.

(v) $0f_{7/2}$, $1p_{3/2}$, $0f_{5/2}$, and $1p_{2/1}$ orbits (0f-1p model space) and the interaction of van Hees [25]) (FPV).

Listed in table 1, are the configuration spaces, isoscalar interactions, and the mass number A of the isobaric multiplets considered in this work.

TABLE 1

List of configuration spaces, isoscalar hamiltonians, and model-space truncations used for each isobaric multiplet

Configuration space	Isoscalar hamiltonian	Mass number A	Model space truncations
0p	CKPOT	10–15	none
pds	RW	14, 15, 17–21	none
1s-0d	W	18–21	none
		22	no more than four particles outside the $0d_{5/2}$ orbit
		34	no more than two holes in the $0d_{5/2}$ orbit
		35–39	none
df	HMW	34–38	none
		39–42	no more than four holes in the $0d_{3/2}$ orbit
		43, 53	no more than two holes in the $0d_{3/2}$ orbit
0f-1p	FPV [a])	42	none
		43, 45, 46, 53, 55	no more than one particle outside the $0f_{7/2}$ orbit
		57, 53	no more than one hole in the $0f_{7/2}$ orbit

[a]) This isoscalar hamiltonian was designed to be used with this model-space truncation.

The many-body wave functions $\psi(\nu, T)$ used to evaluate the one-body and two-body transition densities were obtained with the Oxford-Buenos Aires-MSU shell-model code [26]). In order that the calculation of the TBTD remain tractable, some truncations on the configuration spaces were found to be necessary, and are also listed in table 1. The effects of the model-space truncations on sd-shell nuclei were checked by adding the empirical INC interaction onto the isoscalar hamiltonian, and then obtaining the eigen-energies in proton-neutron formalism (see eqs. (3.3) below) using the full configuration space. The isotopic mass shifts evaluated using perturbation theory within the truncated model space were found to be in good agreement with those obtained with the full-space proton-neutron calculation.

As was mentioned in the introduction, the explicit form of the isovector and isotensor components of the nuclear hamiltonian is unknown, and, therefore, is determined empirically. Here we assume a specific form for $H^{(k)}$ that does not mix isospin in the nucleon-nucleon system, and may be written in terms of the $T=0$ and $T=1$ nucleon-nucleon channels as:

$$H_{\rm tot} = v_0^{(0)} I_0^{(0)} + \sum_{k=0}^{2} v_1^{(k)} I_1^{(k)} ,$$

where the explicit isospin dependence has been separated from the radial and spin components of the nucleon-nucleon interaction with the operators $I_T^{(k)}$, which are given by

$$I_0^{(0)} = \tfrac{1}{4} - \boldsymbol{t}(1) \cdot \boldsymbol{t}(2) ,$$

$$I_1^{(0)} = \tfrac{3}{4} + \boldsymbol{t}(1) \cdot \boldsymbol{t}(2) ,$$

$$I_1^{(1)} = \tfrac{1}{2}(t_z(1) + t_z(2)) ,$$

$$I_1^{(2)} = t_z(1) t_z(2) - \tfrac{1}{3}\boldsymbol{t}(1) \cdot \boldsymbol{t}(2) .$$

With this in mind, we take the $T = 1$ part of the hamiltonian to be of the form

$$v_1^{(k)} = \sum_{\mu} S_{\mu}^{(k)} V_{\mu}(r) , \tag{3.1}$$

where $\mu = C$, π, ρ, and 0. $V_C(r)$ is the Coulomb potential e^2/r, $V_{\pi}(r)$ and $V_{\rho}(r)$ are Yukawa potentials of the form

$$V_{\mu}(r) = \mathrm{e}^{-\mu r}/\mu r ,$$

with $\mu_{\pi} = 0.7\ \mathrm{fm}^{-1}$ and $\mu_{\rho} = 3.9\ \mathrm{fm}^{-1}$, and V_0 represents the $T = 1$ part of the initial isoscalar two-body hamiltonian. The strength of each part of the interaction in eq. (3.1) is embodied in the coefficients $S_{\mu}^{(k)}$.

Before continuing with the formalism necessary to determine the empirical interactions, we note that for the purpose of performing a calculation within proton-neutron formalism it is necessary to express the two-body matrix elements of eq. (3.1) in terms of proton-proton (pp), neutron-neutron (nn), and proton-neutron (pn) two-body matrix elements. This is accomplished by applying eq. (2.2) to the two-nucleon system, and by noting that the doubly reduced two-body matrix elements are given by

$$\langle \rho_i \rho_j ; J, T = 1 \| \| v_1^{(1)} I^{(1)} \| \| \rho_m \rho_n ; J, T = 1 \rangle$$
$$= \{ \tfrac{3}{2}(2J+1) \}^{1/2} \langle \rho_i \rho_j ; J, T = 1 | v_1^{(1)} | \rho_m \rho_n ; J, T = 1 \rangle , \tag{3.2a}$$

$$\langle \rho_i \rho_j ; J, T = 1 \| \| v_1^{(2)} I^{(2)} \| \| \rho_m \rho_n ; J, T = 1 \rangle$$
$$= \{ \tfrac{5}{6}(2J+1) \}^{1/2} \langle \rho_i \rho_j ; J, T = 1 | v_1^{(2)} | \rho_m \rho_n ; J, T = 1 \rangle , \tag{3.2b}$$

where the isospin label on the unreduced matrix elements is preserved as a reminder to apply the Pauli principle, i.e. if $\rho_i = \rho_j$, then $J + T$ is restricted to only odd values. The proton-proton, neutron-neutron, and the $T = 1$ part of the proton-neutron matrix elements are then

$$v_{ijkl;J}^{(\mathrm{pp})} = v_{ijkl;JT=1}^{(0)} + \tfrac{1}{2} v_{ijkl;J,T=1}^{(1)} + \tfrac{1}{6} v_{ijkl;J,T=1}^{(2)} , \tag{3.3a}$$

$$v_{ijkl;J}^{(\mathrm{nn})} = v_{ijkl;JT=1}^{(0)} - \tfrac{1}{2} v_{ijkl;J,T=1}^{(1)} + \tfrac{1}{6} v_{ijkl;J,T=1}^{(2)} , \tag{3.3b}$$

$$v_{ijkl;J}^{(\mathrm{pn})}(T=1) = v_{ijkl;J,T=1}^{(0)} - \tfrac{1}{3} v_{ijkl;J,T=1}^{(2)} , \tag{3.3c}$$

where the shorthand notation $v_{ijkl;J}^{(\mathrm{NN}')}$ represents the nucleon-nucleon matrix element $\langle \rho_i^{\mathrm{N}}, \rho_j^{\mathrm{N}'}; J | H_{\mathrm{tot}} | \rho_k^{\mathrm{N}}, \rho_l^{\mathrm{N}'}; J \rangle$ and $v_{ijkl;J,T}^{(k)}$ represents the isospin-formalism two-body matrix element $\langle \rho_i, \rho_j; J, T | v_1^{(k)} | \rho_k, \rho_l; J, T \rangle$ (see eqs. (3.2)). Including the $T=0$ part of the hamiltonian, the total proton-neutron two-body matrix elements are then given by

$$v_{ijkl;J}^{(\mathrm{pn})} = [\tfrac{1}{2}(1+\delta_{ij})(1+\delta_{kl})]^{1/2} (v_{ijkl;J}^{(\mathrm{pn})}(T=1) + v_{ijkl;J,T=0}^{(0)}) .$$

The proton and neutron single-particle energies are obtained by inverting eqs. (2.7).

Finally, it is also convenient to invert eqs. (3.3) to relate the tensor components of the interaction to the interactions between protons and neutrons:

$$v^{(0)} = \tfrac{1}{3}(v^{(\mathrm{pp})} + v^{(\mathrm{nn})} + v^{(\mathrm{nn})}) , \tag{3.4a}$$

$$v^{(1)} = v^{(\mathrm{pp})} - v^{(\mathrm{nn})} , \tag{3.4b}$$

$$v^{(2)} = v^{(\mathrm{pp})} + v^{(\mathrm{nn})} - 2v^{(\mathrm{pn})} , \tag{3.4c}$$

where eqs. (3.4b) and (3.4c) are commonly referred to as the charge-asymmetric and charge-dependent parts of the nucleon-nucleon interaction, respectively.

In this work, the two-body matrix elements of the Coulomb and Yukawa-like potentials were evaluated using harmonic-oscillator radial wave functions [27]). Harmonic-oscillator wave functions were used in order to simplify the separation into relative and center-of-mass coordinates. We believe that in most cases this is an adequate approximation to a more realistic potential, such as a Woods-Saxon, as long as the oscillator length parameter is chosen to reproduce the experimental rms charge radii. However, in some cases, such as the lower part of the p- and sd-shells, the loose binding of the valence orbits is probably the major source of error in our calculations.

The Coulomb and Yukawa two-body matrix elements and the single-particle energies $\varepsilon^{(1)}(\rho)$ were evaluated for $A=39$ ($\hbar\omega = 11.096$ MeV), and then multiplied by the scaling factor

$$S(A) = \left\{ \frac{\hbar\omega(A)}{11.096} \right\}^{1/2} \tag{3.5}$$

to account for the dependence on A. We note that this factor is exact for evaluating matrix elements of the Coulomb interaction, and is an adequate approximation for the Yukawa-like matrix elements. Short-range correlations (SRC) in the relative wave function were accounted for by including the factor $1+f(r)$ given by Miller and Spencer [28]) ($\alpha = 1.10$ fm^{-2} and $\beta = 0.68$ fm^{-2}).

Values of $\hbar\omega(A)$ can be taken directly from experimental rms charge radii [29]) or from a global parameterization of the data:

$$\hbar\omega(A) = 45A^{-1/3} - 25A^{-2/3} \text{ MeV}. \tag{3.6}$$

A comparison between experimental [30–33]) and parameterized values of $\hbar\omega(A)$ is shown in fig. 1. We found that for $A \leq 50$, eq. (3.5) yielded somewhat better results

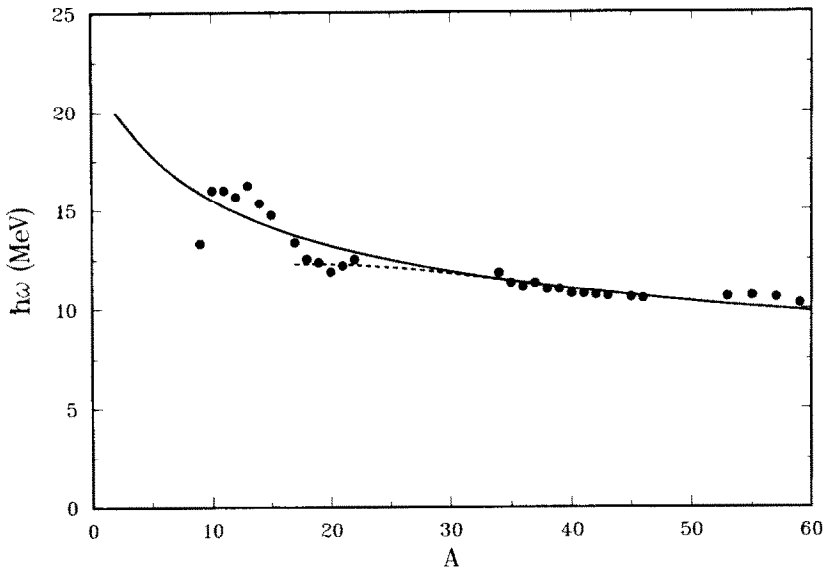

Fig. 1. Comparison between experimental [30-33]) (solid circles) and parameterized (eq. (3.6); solid line) values of $\hbar\omega$. The dashed line indicates the parameterized values of $\hbar\omega$ multiplied by eq. (3.7) that were used for sd-model-space nuclei.

than did the experimentally determined values, while for $A \geq 50$, the experimental values were superior. In addition, it was found that for sd-shell nuclei, better results were obtained using the parameterized values of $\hbar\omega$ multiplied by the additional factor

$$1 - 0.1195 \left(\frac{40 - A}{24} \right)^3 . \tag{3.7}$$

The origin of this correction can be understood from fig. 1, where it is seen that the deviation between experimental and parameterized values of $\hbar\omega$ is larger at the lower end of the sd shell. The additional factor tends to correct for this difference, and is indicated in fig. 1 by the dashed line. In summary, values of $\hbar\omega(A)$ given by eq. (3.6) were used in the 0p, pds, and df model spaces. The product of eqs. (3.6) and (3.7) was used for the 1s-0d model space. While in the fp model space, eq. (3.6) was used for $A < 50$, and the empirically [31-33]) determined values of 10.570*, 10.613*, 10.503*, and 10.222** MeV were used for $A = 53, 55, 57$, and 59, respectively.

Using eqs. (2.4) and (2.6), the b- and c-coefficients can be written as a sum of terms depending on the isovector single-particle energies $\varepsilon^{(1)}(\rho)$ and the strength parameters $S_\mu^{(k)}$. Hence, the b- and c-coefficients for the $(2T+1)$ analog states

* Extrapolated from data in table IV in ref. [31]) and table V of ref. [32]).
** From ref. [33]).

$\psi(\nu, T, T_z)$ $(-T \leq T_z \leq T)$ can be rewritten as

$$b(\nu, T) = \sum_{\rho} \varepsilon^{(1)}(\rho)\delta^{(1)}(\nu, T, \rho) + \sum_{\mu} S_{\mu}^{(1)} \gamma_{\mu}^{(1)}(\nu, T), \tag{3.8a}$$

$$c(\nu, T) = \sum_{\mu} S_{\mu}^{(2)} \gamma_{\mu}^{(2)}(\nu, T), \tag{3.8b}$$

where the quantities $\delta^{(1)}(\nu, T, \rho)$ and $\gamma_{\mu}^{(k)}(\nu, T)$ are given by

$$\delta^{(1)}(\nu, T, \rho) = \left\{ \frac{2(2j_{\rho}+1)}{3(2J+1)T(2T+1)(T+1)} \right\}^{1/2} \mathrm{OBTD}_{\nu,T;\nu,T}(\rho, \rho; 1), \tag{3.9a}$$

$$\begin{aligned} \gamma_{\mu}^{(1)}(\nu, T) = & \left\{ \frac{1}{(2J+1)T(2T+1)(T+1)} \right\}^{1/2} \\ & \times \sum_{ijmn} \mathrm{TBTD}_{\nu,T;\nu T}(\rho_i\rho_j; J, T=1: \rho_m\rho_n; J, T=1; \Delta J=0, k=1) \\ & \times \langle \rho_i\rho_j; J, T=1 \| V_{\mu} I^{(1)} \| \rho_m\rho_n; J, T=1 \rangle, \end{aligned} \tag{3.9b}$$

$$\begin{aligned} \gamma_{\mu}^{(2)}(\nu, T) = & \left\{ \frac{1}{(2J+1)(2T-1)(2T+1)(T+1)(2T+3)} \right\}^{1/2} \\ & \times \sum_{ijmn} \mathrm{TBTD}_{\nu,T;\nu,T}(\rho_i\rho_j; J, T=1: \rho_m\rho_n; J, T=1; \Delta J=0, k=2) \\ & \times \langle \rho_i\rho_j; J, T=1 \| V_{\mu} I^{(2)} \| \rho_m\rho_n; J, T=1 \rangle. \end{aligned} \tag{3.9c}$$

The single-particle energies $\varepsilon^{(1)}(\rho)$ and the strength parameters $S_{\mu}^{(k)}$ can then be determined by performing a least-squares fit to a set of experimental b- and c-coefficients.

Before continuing with a description of the results of the fits, we briefly outline the procedure followed to determine the "best" set of isovector and isotensor parameters. First, we note that it is not a strict requirement that the isovector and isotensor Coulomb strengths be equal since we have not included higher-order Coulomb effects [12]). However, we found that in most cases they were very similar, and, therefore, for the sake of uniformity and simplicity, we have chosen to determine the total hamiltonian while requiring $S_C^{(1)} = S_C^{(2)} = S_C$. Further, we found that only one of the remaining parameters was sufficient to fit the data. Of these, the pion Yukawa required a significant renormalization of the Coulomb strength. On the other hand, the fits including V_{ρ} and V_0 yielded qualitatively similar results, and for the sake of brevity we report those obtained with V_0. The "best" parameter sets were then obtained by first fitting to the b- and c-coefficients separately, and then setting S_C equal to the average value obtained for the two fits. The isovector single-particle energies and the isovector and isotensor coefficients $S_0^{(1)}$ and $S_0^{(2)}$ were then obtained by refitting the experimental data while keeping S_C fixed.

An alternative procedure to that used here would be to perform a least-squares fit to both b- and c-coefficients simultaneously while restricting $S_C^{(1)} = S_C^{(2)}$. The drawback of this method, however, is that since the experimental errors for b- and

c-coefficients are approximately the same, and the b-coefficients are an order of magnitude larger, the b-coefficients would have a larger weight in the fitting procedure.

3.1. FIT TO b-COEFFICIENTS

In this section, the results of the least-squares fit to experimental b-coefficients are presented. Five separate isovector interactions were determined, and the results are given in table 2. The parameter uncertainties and the rms deviation between the fitted and experimental b-coefficients for each fit are also indicated in table 2. The data base for each fit was obtained from the b-coefficients compiled in ref. [19]), the ground-state binding energies tabulated by Wapstra and Audi [34]), the ^{57}Cu mass measurement of Sherrill *et al.* [35]), and the excitation energies compiled by Endt and Van der Leun [36]) and Ajzenberg-Selove [37]). In addition to the restriction $S_C^{(1)} = S_C^{(2)}$, the fits to 0f-1p model-space b-coefficients were performed while requiring that $\varepsilon^{(1)}(0f_{7/2}) = \varepsilon^{(1)}(0f_{5/2}) = \varepsilon^{(1)}(0f)$ and $\varepsilon^{(1)}(1p_{3/2}) = \varepsilon^{(1)}(1p_{1/2}) = \varepsilon^{(1)}(1p)$. This last condition was imposed because of the insensitivity of the experimental data to the single-particle energies $\varepsilon^{(1)}(0f_{5/2})$ and $\varepsilon^{(1)}(1p_{1/2})$. A comparison between experimental b-coefficients and those obtained with the "best" isovector interactions is given in tables 3–7 and figs. 2–6 for the 0p, pds, 1s-0d, df, and 0f-1p shell-model spaces.

TABLE 2

Parameters for the "best" isovector and isotensor interaction for each shell-model configuration space

	Configuration space				
	0p	pds	1s-0d	df	0f-1p
$\varepsilon(0p_{3/2})$ [a])	0.7573 (600)				
$\varepsilon(0p_{1/2})$	0.9805 (1040)	2.5890 (280)			
$\varepsilon(0d_{5/2})$		2.4850 (470)	3.3974 (150)		
$\varepsilon(1s_{1/2})$		2.0433 (660)	3.3113 (480)		
$\varepsilon(0d_{3/2})$			3.3509 (480)	6.2181 (120)	
$\varepsilon(0f_{7/2})$				5.9523 (116)	7.4208 (290)
$\varepsilon(1p_{3/2})$					7.2135 (456)
$\varepsilon(0f_{5/2})$					7.4208 (171)
$\varepsilon(1p_{3/2})$					7.2135 (456)
S_C	1.03 (4)	1.04 (3)	1.00 (2)	1.04 (3)	1.036 (11)
$S_0^{(1)} \times 100$	−4.20 (111)	−4.20 (63)	−1.71 (50)	−1.80 (85)	1.57 (119)
$S_0^{(2)} \times 100$	−1.68 (50)	−2.99 (60)	−4.88 (30)	−5.71 (110)	−4.20 [b])
b rms. (MeV):	70.2	44.2	26.8	21.2	32.9
c rms. (keV):	13.2	15.9	8.6	21.0	

[a]) The single-particle energies are appropriate for $A = 39$.

[b]) This quantity was not fit upon, and was taken to be the value expected from nucleon-nucleon scattering data.

TABLE 3

Comparison between fitted b- and c-coefficients and experimental values for 0p-shell nuclei

A	J^π	T	b (exp) (MeV)	b (fit) (MeV)	c (exp) (keV)	c (fit) (keV)
9	$\frac{3}{2}^-$	$\frac{1}{2}$	1.851 (1)	1.854		
	$\frac{5}{2}^-$	$\frac{1}{2}$	1.783 (5)	1.940		
	$\frac{3}{2}^-$	$\frac{3}{2}$	2.108 (1)	2.150	264 (7)	280
10	0^+	1	2.330 (1)	2.286	363 (1)	368
	2^+	1	2.323 (1)	2.329	300 (1)	310
11	$\frac{3}{2}^-$	$\frac{1}{2}$	2.765 (2)	2.691		
	$\frac{1}{2}^-$	$\frac{1}{2}$	2.640 (2)	2.643		
12	1^+	1	2.767 (1)	2.754	244 (3)	235
	2^+	1	2.770 (1)	2.743	204 (6)	220
13	$\frac{1}{2}^-$	$\frac{1}{2}$	3.003 (3)	2.849		
	$\frac{3}{2}^-$	$\frac{1}{2}$	2.829 (2)	2.893		
	$\frac{1}{2}^-$	$\frac{3}{2}$	2.965 (10)	3.034	257 (3)	261
14	0^+	1	3.276 (1)	3.229	337 (1)	315
15	$\frac{1}{2}^-$	$\frac{1}{2}$	3.536 (1)	3.603		
	$\frac{3}{2}^-$	$\frac{1}{2}$	3.388 (1)	3.384		

As can be seen from tables, generally good results (rms deviations ≤ 30 keV) were obtained in the sd, df, and fp shell-model spaces. The somewhat poorer results obtained in the p-shell and the pds-space are most likely due to the loosely bound nature of some states in these light nuclei. For these cases, the harmonic-oscillator assumption for the radial wave functions is inadequate. This is particularly true for the $1s_{1/2}$ orbit because of the absence of a centrifugal barrier. In addition, these light nuclei are also prone to multi-particle breakup, indicating that clustering effects may also be important.

Although the results of the fits to sd-shell nuclei are generally good, it should be pointed out that the fitted isovector single-particle energies extrapolated to $A = 17$ yield a b-coefficient for the $\frac{1}{2}^+$ state, $b_{\rm fit}(\frac{1}{2}^+) = 3.477$ MeV, that is not in good agreement with the experimental value of 3.168 MeV, as determined from ^{17}F and ^{17}O [refs. [34,37])]. The tendency for the experimental value to be smaller is again most likely due to the fact that this level is loosely bound relative to ^{16}O, and, therefore, has a larger rms radius and a smaller Coulomb energy. On the other hand, the theoretical b-coefficients for the $\frac{5}{2}^+$ and $\frac{3}{2}^+$ states, $b_{\rm fit}(\frac{5}{2}^+) = 3.519$ MeV, $b_{\rm fit}(\frac{3}{2}^+) = 3.567$ MeV, are in reasonable agreement with the experimental values of 3.543 MeV and 3.561 MeV, respectively. We remark, however, that because of the loosely bound nature of these $A = 17$ states, they were not included in the fit to sd-shell b-coefficients. In addition, the surprisingly good agreement between the fitted and experimental values for the $\frac{5}{2}^+$ and $\frac{3}{2}^+$ states is primarily due to the parameterized value of $\hbar\omega$ modified by eq. (3.7), whereas the $\hbar\omega$ determined from the rms charge radius yields fitted b-coefficients that are in considerable disagreement with experiment. This is

TABLE 4

Comparison between fitted b- and c-coefficients and experimental values for pds-space nuclei

A	J^π	T	b (exp) (MeV)	b (fit) (MeV)	c (exp) (keV)	c (fit) (keV)
14	0^+	1	3.276 (1)	3.260	337 (1)	327
15	$\frac{1}{2}^-$	$\frac{1}{2}$	3.536 (1)	3.532		
	$\frac{1}{2}^+$	$\frac{1}{2}$	3.420 (2)	3.408		
	$\frac{5}{2}^+$	$\frac{1}{2}$	3.507 (1)	3.486		
	$\frac{1}{2}^+$	$\frac{3}{2}$	3.081 (43)	3.209	227 (22)	250
17	$\frac{5}{2}^+$	$\frac{1}{2}$	3.543 (1)	3.604		
	$\frac{1}{2}^-$	$\frac{1}{2}$	3.592 (1)	3.529		
	$\frac{1}{2}^+$	$\frac{3}{2}$	3.657 (1)	3.712	238 (7)	253
18	0^+	1	3.833 (3)	3.845	354 (3)	341
	2^+	1	3.785 (3)	3.743	268 (3)	294
	4^+	1	3.744 (3)	3.781	209 (3)	200
	1^-	1	3.865 (5)	3.875		
19	$\frac{1}{2}^+$	$\frac{1}{2}$	4.021 (1)	4.007		
	$\frac{1}{2}^-$	$\frac{1}{2}$	4.186 (1)	4.262		
	$\frac{5}{2}^+$	$\frac{1}{2}$	4.062 (6)	4.032		
	$\frac{5}{2}^+$	$\frac{3}{2}$	3.981 (4)	4.000	239 (5)	240
20	2^+	1	4.211 (4)	4.201	198 (4)	190
	3^+	1	4.197 (4)	4.150	191 (6)	216
	4^+	1	4.184 (4)	4.175	166 (6)	188
21	$\frac{5}{2}^+$	$\frac{1}{2}$	4.310 (3)	4.312		
	$\frac{1}{2}^+$	$\frac{1}{2}$	3.958 (3)	4.006		
	$\frac{1}{2}^-$	$\frac{1}{2}$	4.344 (3)	4.305		
	$\frac{5}{2}^+$	$\frac{3}{2}$	4.441 (3)	4.395	244 (3)	232
	$\frac{1}{2}^+$	$\frac{3}{2}$	4.412 (5)	4.400	230 (6)	226

again a manifestation of the relatively low binding energy of the closed-core plus particle systems, and represents a limitation of our model. Further, it is perhaps clear from this example that single-particle energies determined from these closed-core plus particle states are not necessarily appropriate for nuclei in the middle or the end of the shell.

In all the configuration spaces, a charge-asymmetric interaction improved the quality of the fits, with the sign being such that $v^{(nn)}$ is more attractive than $v^{(pp)}$ for all but the 0f-1p shell-model space. This charge-asymmetric interaction, however, can partly be interpreted as being an effect due to differences between proton and neutron radial wave functions (radial-wave function (RWF) correction). Coulomb repulsion tends to push proton radial-wave functions out relative to neutrons, and, therefore, matrix elements of $v^{(nn)}$ will be larger (more attractive) than those of $v^{(pp)}$ even if $v^{(pp)} = v^{(nn)}$. This effect can be particularly important for light nuclei because of their loosely bound nature. Lawson [12]) has estimated the RWF corrections for the 0p shell by assuming that the Cohen–Kurath two-body matrix elements are effected in the same manner as a δ-function potential. With this assumption, he

TABLE 5

Comparison between fitted b- and c-coefficients and experimental values for 1s-0d-shell nuclei

A	J^π	T	b (exp) (MeV)	b (fit) (MeV)	c (exp) (keV)	c (fit) (keV)
18	0^+	1	3.833 (5)	3.841	354 (3)	365
	2^+	1	3.875 (5)	3.791	268 (3)	281
19	$\frac{1}{2}^+$	$\frac{1}{2}$	4.021 (1)	4.056		
	$\frac{5}{2}^+$	$\frac{1}{2}$	4.062 (6)	4.068		
	$\frac{3}{2}^+$	$\frac{1}{2}$	4.003 (5)	4.048		
	$\frac{5}{2}^+$	$\frac{3}{2}$	3.984 (5)	3.993	239 (2)	240
	$\frac{3}{2}^+$	$\frac{3}{2}$	3.988 (5)	3.989	230 (6)	238
20	2^+	1	4.211 (4)	4.208	186 (4)	190
	3^+	1	4.179 (4)	4.194	191 (6)	211
	4^+	1	4.184 (4)	4.188	166 (6)	180
21	$\frac{3}{2}^+$	$\frac{1}{2}$	4.329 (3)	4.347		
	$\frac{5}{2}^+$	$\frac{1}{2}$	4.310 (3)	4.333		
	$\frac{5}{2}^+$	$\frac{3}{2}$	4.441 (3)	4.402	244 (3)	234
	$\frac{1}{2}^+$	$\frac{3}{2}$	4.411 (3)	4.403	230 (4)	228
22	0^+	1	4.597 (2)	4.566	316 (2)	307
	2^+	1	4.583 (3)	4.559	282 (2)	268
	2^+	1	4.573 (3)	4.558	235 (2)	228
	4^+	1	4.573 (3)	4.548	235 (2)	235
34	0^+	1	6.559 (2)	6.546	284 (2)	277
	2^+	1	6.541 (2)	6.521	235 (2)	225
	2^+	1	6.551 (2)	6.530	235 (2)	237
	0^+	1	6.537 (2)	6.518	196 (2)	199
35	$\frac{3}{2}^+$	$\frac{1}{2}$	6.747 (1)	6.746		
	$\frac{1}{2}^+$	$\frac{1}{2}$	6.712 (1)	6.672		
	$\frac{5}{2}^+$	$\frac{1}{2}$	6.734 (1)	6.723		
	$\frac{3}{2}^+$	$\frac{1}{2}$	6.654 (1)	6.673		
	$\frac{5}{2}^+$	$\frac{1}{2}$	6.768 (10)	6.664		
	$\frac{1}{2}^+$	$\frac{1}{2}$	6.664 (12)	6.652		
	$\frac{3}{2}^+$	$\frac{3}{2}$	6.666 (2)	6.667	199 (2)	199
36	2^+	1	6.830 (4)	6.829	146 (4)	139
	3^+	1	6.836 (9)	6.831	214 (9)	225
	1^+	1	6.805 (9)	6.814	188 (9)	197
	0^+	2	6.828 (3)	6.834	201 (2)	201
37	$\frac{3}{2}^+$	$\frac{1}{2}$	6.931 (1)	6.908		
	$\frac{1}{2}^+$	$\frac{1}{2}$	6.890 (2)	6.911		
	$\frac{5}{2}^+$	$\frac{1}{2}$	6.885 (2)	6.952		
	$\frac{1}{2}^+$	$\frac{3}{2}$	6.984 (6)	6.996	197 (6)	201
	$\frac{3}{2}^+$	$\frac{3}{2}$	6.945 (12)	6.960	211 (9)	217
38	0^+	1	7.110 (3)	7.109	284 (3)	286
	2^+	1	7.129 (4)	7.160	199 (3)	198
39	$\frac{3}{2}^+$	$\frac{1}{2}$	7.313 (2)	7.321		
	$\frac{1}{2}^+$	$\frac{1}{2}$	7.259 (2)	7.279		

TABLE 6

Comparison between fitted b- and c-coefficients and experimental values for df-space nuclei

A	J^π	T	b (exp) (MeV)	b (fit) (MeV)	c (exp) (keV)	c (fit) (keV)
34	0^+	1	6.559 (2)	6.552	284 (2)	283
	2^+	1	6.541 (2)	6.509	235 (2)	184
36	2^+	1	6.830 (4)	6.838	146 (4)	127
	3^+	1	6.836 (9)	6.836	214 (9)	226
	1^+	1	6.805 (9)	6.832	188 (9)	224
	0^+	2	6.828 (3)	6.830	201 (2)	196
37	$\frac{3}{2}^+$	$\frac{1}{2}$	6.931 (1)	6.940		
	$\frac{3}{2}^+$	$\frac{3}{2}$	6.984 (1)	6.989	197 (6)	195
38	0^+	1	7.110 (3)	7.107	284 (3)	279
	2^+	1	7.129 (3)	7.151	199 (6)	182
	3	1	7.052 (4)	6.984		
39	$\frac{3}{2}^+$	$\frac{1}{2}$	7.313 (2)	7.305		
	$\frac{3}{2}^-$	$\frac{1}{2}$	7.318 (2)	7.308		
	$\frac{7}{2}^-$	$\frac{1}{2}$	7.295 (2)	7.294		
40	4^-	1	7.286 (2)	7.302	157 (3)	161
	3^-	1	7.288 (2)	7.302	153 (3)	139
	2^-	1	7.272 (2)	7.302	178 (3)	205
	5^-	1	7.289 (2)	7.302	157 (3)	173
41	$\frac{7}{2}^-$	$\frac{1}{2}$	7.277 (2)	7.292		
42	0^+	1	7.495 (3)	7.482	289 (3)	273
43	$\frac{7}{2}^-$	$\frac{1}{2}$	7.650 (7)	7.634		
53	$\frac{7}{2}^-$	$\frac{1}{2}$	9.086 (18)	9.069		

TABLE 7

Comparison between fitted b-coefficients and experimental values for 0f-1p-shell nuclei

A	J^π	T	b (exp) (MeV)	b (fit) (MeV)
42	0^+	1	7.495 (3)	7.508
	2^+	1	7.510 (3)	7.504
	4^+	1	7.458 (3)	7.503
	6^+	1	7.422 (3)	7.405
43	$\frac{7}{2}^-$	$\frac{1}{2}$	7.650 (7)	7.663
45	$\frac{7}{2}^-$	$\frac{1}{2}$	7.914 (18)	7.916
	$\frac{3}{2}^-$	$\frac{1}{2}$	7.934 (27)	7.900
	$\frac{5}{2}^-$	$\frac{1}{2}$	7.930 (27)	7.919
46	0^+	1	8.109 (15)	8.061
53	$\frac{7}{2}^-$	$\frac{1}{2}$	9.086 (18)	9.102
55	$\frac{7}{2}^-$	$\frac{1}{2}$	9.473 (10)	9.460
57	$\frac{3}{2}^-$	$\frac{1}{2}$	9.519 (130)	9.601
59	$\frac{3}{2}^-$	$\frac{1}{2}$	9.876 (40)	9.904

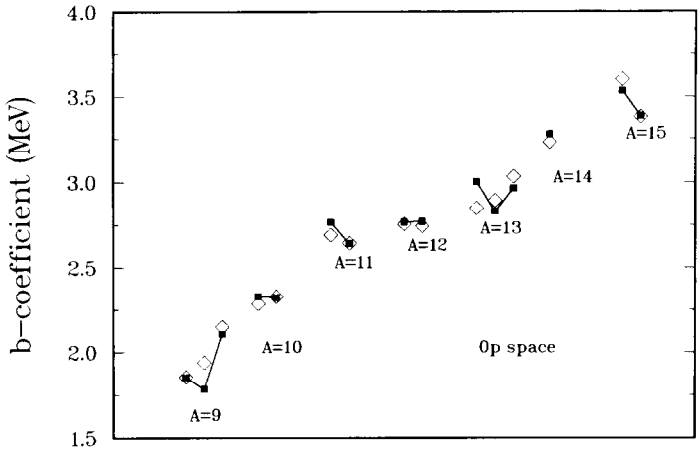

Fig. 2. Plot of 0p-model-space b-coefficients. Experimental data are represented by filled squares, and are connected by the solid line for each isomultiplet, while the fitted values are given by the open diamonds. The coefficients are plotted in the same order as they appear in table 3.

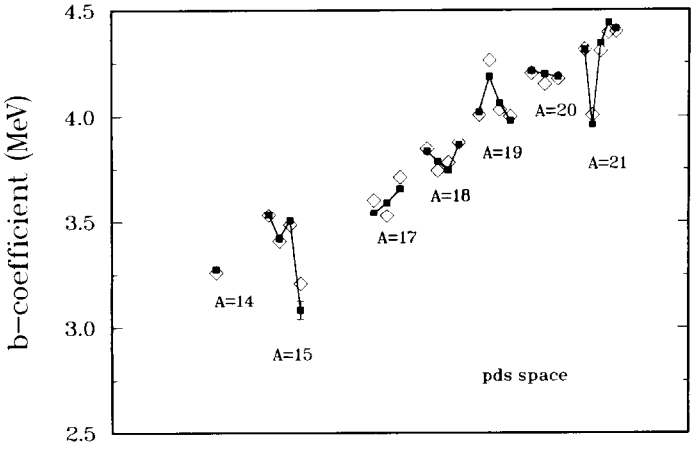

Fig. 3. Same as fig. 2 for the pds-model space b-coefficients. The coefficients are plotted as they appear in table 4.

finds that the neutron-neutron two-body matrix element $\langle(0p_3/2)^2; J = 0|V|(0p_{3/2})^2; J = 0\rangle$ is 5.6% larger than the proton-proton matrix element. The value −4% obtained with the fitting procedure here is not inconsistent with these results. Unfortunately, it is difficult in general to determine precisely how much of the fitted charge asymmetry is due to the RWF correction or the presence of a real charge-asymmetric two-body interaction.

The presence of a small charge-asymmetric potential, however, is consistent with the work of Negle [8]), Sato [9]), and Shlomo [10]), where it was found (using different

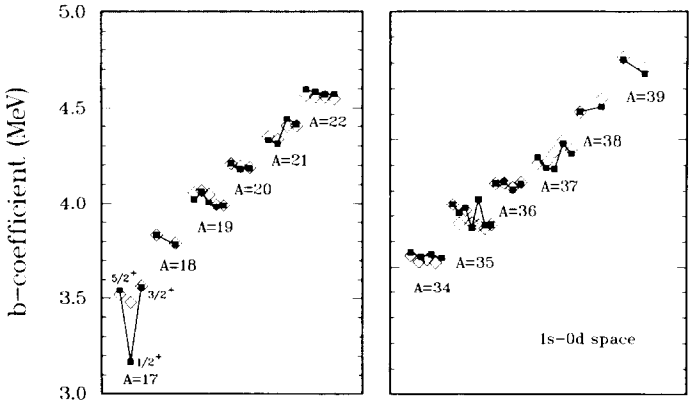

Fig. 4. Same as fig. 2 for the 0s-1d-model space b-coefficients. The coefficients are plotted as they appear in table 5.

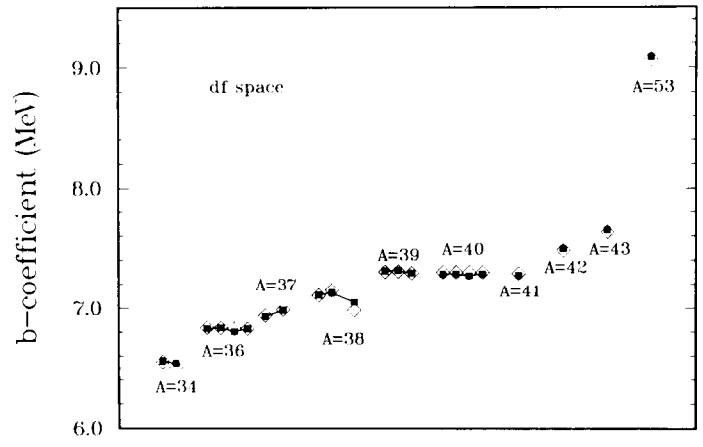

Fig. 5. Same as fig. 2 for the df-model space b-coefficients. The coefficients are plotted as they appear in table 6.

models than in the present work) that a small (approximately -1%) phenomenological charge-asymmetric interaction could account for at least part of the Nolen-Schiffer anomaly. As was mentioned in the introduction, however, there is at present no fundamental theoretical model for such an interaction. In addition, a recent analysis of nucleon-nucleus scattering data by Winfield *et al.* [38]) indicates that the nucleon-nucleon interaction between neutrons might be slightly more attractive than it is for protons. Their results, however, do not rule out $v^{(pp)} = v^{(nn)}$. Finally, these studies are not contradicted by free nucleon-nucleon scattering data. The neutron-neutron and proton-proton scattering lengths are $a^{(nn)} = -18.6 \pm 0.5$ fm [ref. [39])] and $a^{(pp)} = -17.1 \pm 1.0$ fm [ref. [40])] (corrected for electromagnetic effects; the in error $a^{(pp)}$ primarily reflects the uncertainty in this correction). The change

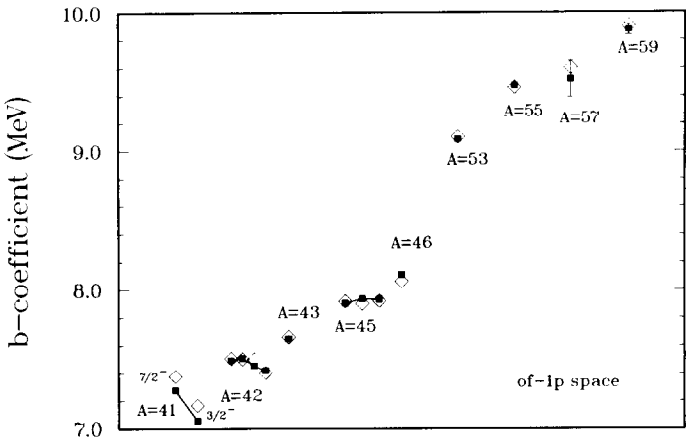

Fig. 6. Same as fig. 2 for the 0f-1p-model space b-coefficients. The coefficients are plotted as they appear in table 7.

in the potential ΔV is related to the change in the scattering length, Δa, for Yukawa potentials by [2])

$$\frac{\Delta a}{a} \approx 14 \frac{\Delta V}{V} . \tag{3.10}$$

Using this relation, the proton-proton and neutron-neutron scattering lengths indicate that $v^{(nn)}$ is $(0.6 \pm 0.4)\%$ more attractive than $v^{(pp)}$.

Another property of the fits is that in some cases a renormalization of the Coulomb strength was needed in order to reduce the rms deviation between fitted and experimental values. A small renormalization the Coulomb strength, however, is not unreasonable, as a number of corrections to the simple $1/r$ potential are expected. These are primarily due to neglecting higher-order Coulomb effects [see ref. [12]) and references contained therein] and the fact that harmonic-oscillator wave functions were used.

3.2. FIT TO c-COEFFICIENTS

In this section, results of the least squares fit to experimental c-coefficients are presented. Fits to 0f-1p shell nuclei were not performed because there is little experimental data in this region. However, the proton-neutron scattering length, $a^{(pn)} = -23.715 \pm 0.015$ fm [ref. [2])], indicates that the isotensor interaction can be parameterized by

$$H^{(2)} = V_C - 0.042(12) V_0 , \tag{3.11}$$

or that $v^{(pn)}$ is approximately 2% more attractive than the average of the proton-proton and neutron-neutron interactions.

The data base for the fits was again determined from the data compilations listed in sect. 3.1. The resulting parameters and rms deviations between theory and experiment are listed in table 2. A comparison between the fitted and experimental values are given in tables 3–6 and figs. 7–10 for the 0p, pds, 1s-0d, and df model spaces. We find that a charge-dependent interaction is necessary in order to reduce the rms deviation between fitted and experimental values, and that the results are generally consistent with the parameterization given by eq. (3.11). The somewhat smaller value obtained for p-shell nuclei may again be due to binding energy effects. Further, the qualitatively similar results obtained while fitting on either $S_p^{(2)}$ and

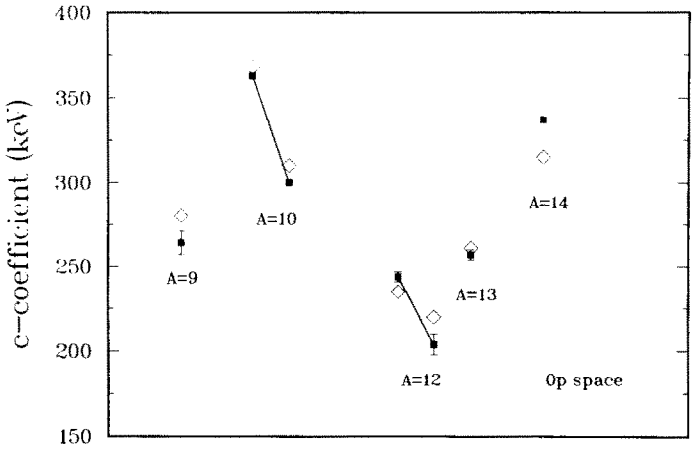

Fig. 7. Plot of 0p-model-space c-coefficients. Experimental data are represented by filled squares, and are connected by the solid line for each isomultiplet, while the fitted values are given by the open diamonds. The coefficients are plotted in the same order as they appear in table 3.

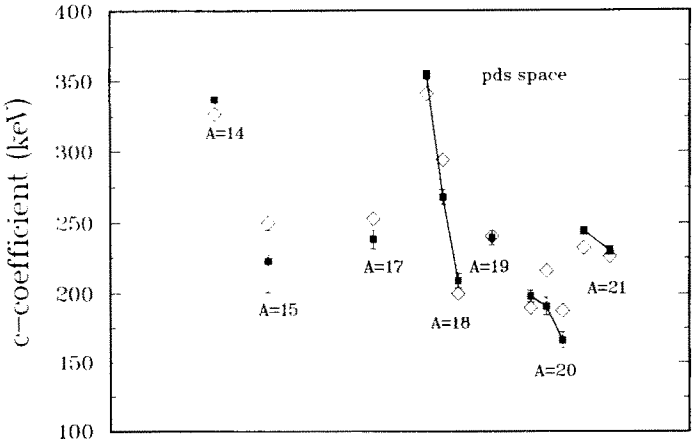

Fig. 8. Same as fig. 7 for the pds-model space c-coefficients. The coefficients are plotted as they appear in table 4.

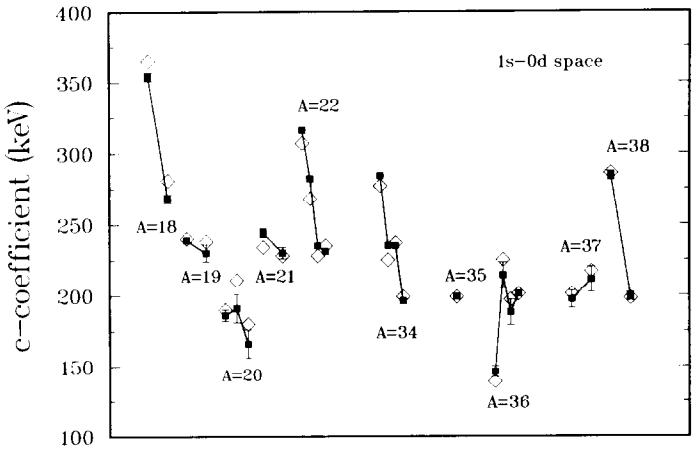

Fig. 9. Same as fig. 7 for the 0s-1d-model space c-coefficients. The coefficients are plotted as they appear in table 5.

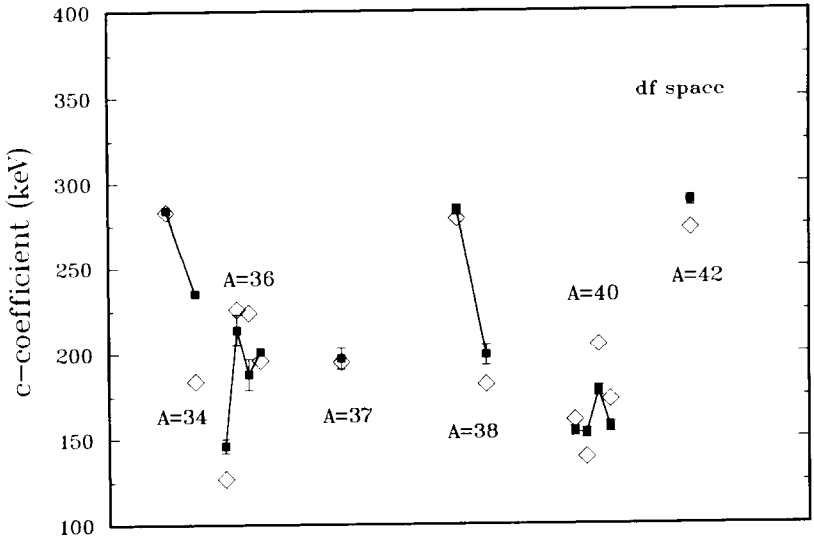

Fig. 10. Same as fig. 7 for the df-model space c-coefficients. The coefficients are plotted as they appear in table 6.

$S_0^{(2)}$ is due to the fact that the isoscalar hamiltonian is generally short range in character, and indicates that the charge-dependent interaction is predominantly a short-range force. This finding is consistent with those of Lawson [12]).

4. Discussion and summary

In this work, isospin-nonconserving interactions were determined for the 0p, pds, 1s-0d, df-, and 0f-1p shell-model configuration spaces by imposing the

requirement that these interactions reproduce experimental b- and c-coefficients of the isobaric-mass-multiplet equation. The empirical hamiltonians reproduce the experimental data rather well for the heavier nuclei, i.e. 0s-1d, df, and 0f-1p-space nuclei. The somewhat poorer results obtained for 0p-space and pds-space nuclei are most likely attributable to the fact that several states in these nuclei are rather loosely bound to nucleon emission.

A general feature of the fits to b-coefficients is that the inclusion of a charge-asymmetric interaction reduced the rms deviation between theory and experiment. Unfortunately, it is difficult to determine exactly how much of the empirical interaction is due to the radial-wave-function correction to the matrix elements of the nucleon-nucleon interaction, or to a charge asymmetry in the interaction itself.

In the fits to the c-coefficients, a charge-dependent interaction was essential in order to fit the data. In addition, it was found that with the exception of the 0p space, the empirically determined interactions were in general agreement with the results expected from the nucleon-nucleon scattering data, i.e. $v^{(pn)}$ is 2% more attractive than the average of $v^{(pp)}$ and $v^{(nn)}$.

The results reported here are generally consistent with those of previous works along these lines [11-14]), i.e. an isovector and isotensor nucleon-nucleon interaction is necessary to reproduce the experimental isotopic mass shifts. In each work, an empirical approach was taken in order to gain some insight into the nature of these potentials and to determine matrix elements that are useful for shell-model calculations, the latter of which was the primary motivation for the present work.

Considerable theoretical work, however, must still be done in order to understand these empirical interactions within a more fundamental basis. As has been mentioned, there is still no model for a charge-asymmetric interaction that can account for the observed b-coefficients, although at least part of the empirical interactions developed here must be due to the radial-wave-function correction. As for the charge-dependent component, a perturbative calculation [41]) of the nucleon-nucleon scattering length based on charge-dependent effects in two-pion exchange, pion-gamma exchange, and pionic mass differences in one-pion exchange can reproduce the differences observed in $a^{(pn)}$ and $a = \frac{1}{2}(a^{(pp)} + a^{(nn)})$. A potential based on these effects, however, is rather complex, and has not yet been applied to a calculation of c-coefficients.

In addition, there is a strong evidence that ground-state correlations (GSC) contribute significantly to the rms charge radius [42,43]). In ^{40}Ca the GSC contribution to the rms radius is estimated [44]) to be approximately 5% of the experimental value. With such a large contribution to the rms charge radius, it is possible that these correlations will also affect the isotopic mass differences [45]), and certainly warrants further investigation.

Finally, we note that the empirical interactions developed here have been used to calculate the corrections to the Fermi matrix element for superallowed β-decay [46]) and the isospin-forbidden spectroscopic amplitudes for the decay of $T = \frac{3}{2}$ states via

proton and neutron emission to $T = 0$ states [47]). Investigations such as those pertaining to isospin-forbidden Fermi β-transitions and β-delayed two proton emission are planned.

This work was supported in part by the National Science Foundation Grant No. PHY-83-12245 and by the Danish Natural Sciences Research Council. W.E.O would like to thank the National Superconducting Cyclotron Laboratory for support during his graduate studies, from which this work originated.

References

1) W. Heisenberg, Z. Phys. **77** (1932) 1
2) E.M. Henley, Isospin in nuclear physics, ed. D.H. Wilkinson (North-Holland, Amsterdam, 1969)
3) J.F. Wilkerson, R.E. Anderson, T.B. Clegg, E.J. Ludwig and W.J. Thompson, Phys. Rev. Lett. **51** (1983) 2269
4) S. Raman, T.A. Walkiewicz and H. Behrens, At. Data Nucl. Data Tables **16** (1975) 451
5) M.D. Cable *et al.*, Phys. Rev. **C30** (1984) 1276
6) J.A. Nolen and J.P. Schiffer, Ann. Rev. Nucl. Sci. **19** (1969) 471
7) N. Auerbach, Phys. Reports **98** (1983) 273
8) J.W. Negele, Nucl. Phys. **A165** (1971) 305
9) H. Sato, Nucl. Phys. **A266** (1976) 269
10) S. Shlomo, Rep. Prog. Phys. **41** (1978) 957
11) R. Sherr and I. Talmi, Phys. Lett. **B56** (1975) 212;
R. Sherr, Phys. Rev. **C16** (1977) 1159
12) R.D. Lawson, Phys. Rev. **C19** (1979) 2359
13) B.A. Brown and R. Sherr, Nucl. Phys. **A322** (1979) 61
14) R.R. Whitehead, A. Watt, D. Kelvin, and H.J. Rutherford, Phys. Lett. **B65** (1976) 323
15) I.S. Towner, J.C. Hardy and M. Harvey, Nucl. Phys. **A284** (1977) 269;
D.H. Wilkinson, Phys. Lett. **B51** (1983) 2269
16) E.P. Wigner, Proc. of the Robert A. Welsch Conference on chemical research (R.A. Welsch Foundation, Houston Texas, 1957) vol. 1, p. 67
17) A.R. Edmonds, Angular momentum in quantum mechanics (Princeton Univ. Press, Princeton, 1960)
18) W. Benenson and E. Kashy, Rev. Mod. Phys. **51** (1979) 527
19) M.S. Anthony, J. Britz, J.R. Bueb and A. Pape, At. Data Nucl. Data Tables **33** (1985) 447
20) P.J. Brussaard and P.W.M. Glaudemans, Shell-model applications in nuclear spectroscopy, (North-Holland, Amsterdam, 1977)
21) S. Cohen and D. Kurath, Nucl. Phys. **A73** (1965) 1
22) B. Reehal and B.H. Wildenthal, Particles and Nuclei **6** (1973) 974
23) B.H. Wildenthal, Prog. Part. Nucl. Phys., ed. D.H. Wilkinson (Pergamon, Oxford, 1984) vol. 11, p. 5
24) S.T. Hseih, X. Ji, R.B.M. Mooy and B.H. Wildenthal, Proc. AIP Conf. on nuclear structure at high spin, excitation and momentum transfer, ed. H. Nann (Am. Inst. of Phys., New York, 1986) p. 357; Bull. of the American Physical Society **30** (1985) 731
25) A.G.M. van Hees and P.W.M. Glaudemans, Z. Phys. **A303** (1981) 267
26) W.D.M. Rae, A. Etchegoyen and B.A. Brown, OXBASH, The Oxford-Buenos Aires-MSU shell-model code, Michigan State University Cyclotron Laboratory Report #524
27) R.D. Lawson, Theory of the nuclear shell model, (Clarendon, Oxford, 1980)
28) G.A. Miller and J.E. Spencer, Ann. of Phys. **100** (1976) 562
29) B.A. Brown, W. Chung and B.H. Wildenthal, Phys. Rev. **C22** (1980) 774
30) B.A. Brown, C.R. Bronk and P.E. Hodgson, J. of Phys. **G10** (1984) 1683;
C.W. Jager, H. de Vries and C. de Vries, At. Nucl. Data Tables **14** (1974) 479;

E. Bergman *et al.*, Proc. Int. Conf. on nuclear physics (Berkeley 1980) p. 110;
J. Kowalski *et al.*, Z. Phys. **A290** (1979) 345
31) H.D. Wolfahrt *et al.*, Phys. Rev. **C23** (1981) 533
32) H.D. Wolfahrt *et al.*, Phys. Rev. **C22** (1980) 264
33) B. Sherrill *et al.*, Phys. Rev. **C28** (1983) 1712
34) A.H. Wapstra and G. Audi, Nucl. Phys. **A432** (1985) 1
35) B. Sherrill *et al.*, Phys. Rev. **C31** (1985) 875
36) P.M. Endt and C. van der Leun, Nucl. Phys. **A310** (1978) 1
37) F. Ajzenberg-Selove, Nucl. Phys. **A375** (1982) 1; **A392** (1983) 1; **A413** (1984) 1; **A433** (1985) 1; **A449** (1986) 1
38) J.S. Winfield, S.M. Austin, R.P. DeVito, U.E.P. Berg, Z. Chen and W. Sterrenburg, Phys. Rev. **C33** (1986) 1
39) B. Gabioud *et al.*, Phys. Lett. **B103** (1981) 9
40) E.M. Henley, Proc. Int. Conf. on few particle problems in the nuclear interaction, Los Angeles, 1972
41) T.E.O. Ericson and G.A. Miller, Phys. Lett. **B132** (1983) 32
42) H. Esbebsen and G.F. Bertsch, Phys. Rev. **C28** (1983) 355
43) F. Barranco and R.A. Broglia, Phys. Lett. **B151** (1985) 90;
44) F. Barranco and R.A. Broglia, Phys. Rev. Lett. **59** (1987) 2724
45) S. Shlomo, Texas A & M preprint #CTP-TAMU-15/86
46) W.E. Ormand and B.A. Brown, Nucl. Phys. **A440** (1985) 274; Proc. Int. Symp. on weak and electromagnetic interactions in nuclei, Heidelberg, July 1-5, 1986, ed. H.V. Klapdor, (Springer, Berlin, 1987) p. 545
47) W.E. Ormand and B.A. Brown, Phys. Lett. **B174** (1986) 128